Recent CMS Results on Heavy Quarks and Hadrons

Alice Bean for the CMS Collaboration

University of Kansas, Lawrence, KS 66045, United States

Using dedicated dimuon triggers with the CMS detector, several results are presented from data collected during 2010, 2011, and 2012. Polarization measurements are shown for the J/Ψ and Υ states. A search for states decaying to $\Upsilon(1S)\pi^+\pi^-$ is presented. The Λ_b^0 lifetime has been measured. An observation of the decay $B_S \to \mu^+\mu^-$ decay is presented.

1 Introduction

Studies of the b-quark are key to understanding the nature of the strong force.[1] The heavy-quark expansion model of nonperturbative quantum chromodynamics provides a framework for predicting properties of b-hadrons. Here, the heavy quarks in the meson move at non-relativistic speeds, so the relativistic corrections are small. The CMS Collaboration has previously published b-hadron production cross section results for: $pp \to \Lambda_b X \to J/\Psi\Lambda X$ [2], $pp \to B^+X$ [3], $pp \to B^0X$ [4], and $pp \to B_S X \to J/\Psi\phi X$ [5]. Figure 1 shows these results compared to Monte Carlo simulations using the Monte Carlo at Next to Leading Order (MC@NLO)/POWHEG [6] generator. The properties of quarkonia states such as J/Ψ, $J/\Psi(2S)$, and $\Upsilon(nS)$, have also been predicted with NRQCD [7].

The CMS Collaboration has recorded proton-proton data at the Large Hadron Collider during 2010, 2011, and 2012. During 2010 and 2011, the center of mass energy was 7 TeV and during 2012, data were taken at 8 TeV. The central feature of the CMS apparatus [8] is a superconducting solenoid of 6 m internal diameter. A tracker, consisting of silicon pixel and silicon strip layers, is immersed in a 3.8 T axial magnetic field of the superconducting solenoid. The pixel tracker consists of three barrel layers and two endcap disks at each barrel end. The strip tracker has 10 barrel layers and 12 endcap disks at each barrel end. The tracker provides an impact parameter resolution of $\sim$15μm and a transverse momentum p_T resolution of about 1.5% for 100 GeV particles. Muons are measured in gas-ionisation detectors that are embedded in the steel return yoke outside the solenoid. In the barrel, there is a drift tube system interspersed with resistive plate chambers, and in the endcaps there is a cathode strip chamber system, also interspersed with resistive plate chambers. The CMS experiment uses a right-handed coordinate system, with the origin at the nominal interaction point, the x axis pointing towards the center of the LHC ring, the y axis pointing up (perpendicular to the plane of the LHC ring), and the z axis along the anticlockwise-beam direction. The polar angle θ is measured from the positive z axis and the pseudorapidity is defined by $\eta = -\ln[\tan(\theta/2)]$. The azimuthal angle ϕ is measured from the positive x axis in the plane perpendicular to the beam.

Decay channels with muons are measured well in the detector. For the results presented here, the muon triggers were used to select events. As the data-taking has progressed, the

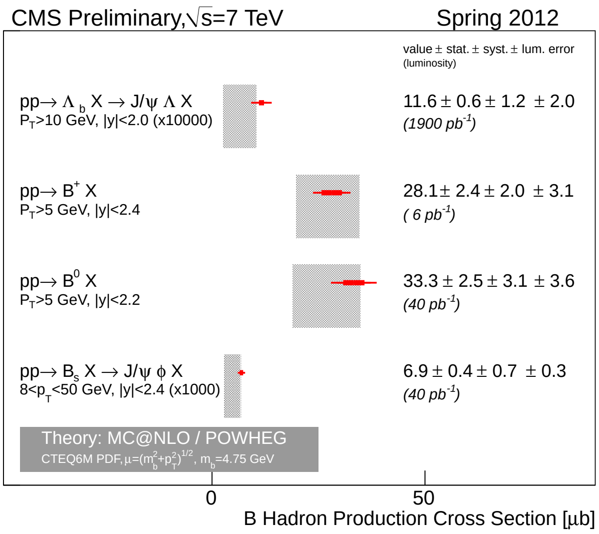

Figure 1: Summary of b-hadron cross section measurements performed by CMS with 7 TeV p-p collision at LHC. The inner error bars of the data points correspond to the statistical uncertainty, whil the outer (thinner) error bars correspond to the quadratic sum of statistical and systematic uncertainties. The outermost brackets correspond to the total error, including a luminosity uncertainty which is also added in quadrature.

collider has continued to improve on the luminosity and the earlier low values of the transverse muon momenta p_T for these triggers have been raised thus limiting the bandwidth for the later datasets for B-physics studies. For proton-proton collisions at a center of mass energy of 7 TeV, the $\Upsilon(1S)$, $\Upsilon(2S)$, and $\Upsilon(3S)$ cross sections are measured as a function of the dimuon transverse momentum and rapidity. A search for the decay $X_b \to \Upsilon(1S)\pi^+\pi^-$, with $\Upsilon(1S) \to \mu^+\mu^-$ is presented. The angular distributions are examined for the J/Ψ, $\Psi(2S)$, $\Upsilon(1S)$, $\Upsilon(2S)$, and $\Upsilon(3S)$ to determine their polarizations. The Λ_b^0 lifetime is measured. Finally, the $B_s \to \mu^+\mu^-$ branching ratio is measured.

2 Cross section measurements for $\Upsilon(nS)$ states

Quarkonium production in hadron collisions is still not well understood [9]. Using 35.8 ± 1.4 pb^{-1} of data taken at a center of mass energy of 7 TeV, the $\Upsilon(1S)$, $\Upsilon(2S)$, and $\Upsilon(3S)$ production cross sections were measured. Their decays to dimuons were used. The product of the $\Upsilon(nS)$ differential cross section and the dimuon branching fraction is determined from the signal yield determined from an extended unbinned maximum likelihood fit to the dimuon invariant mass spectrum, corrected by the acceptance and the efficiency. After integrating over the Υ transverse momentum range $p_T <$ 50 GeV/c and rapidity range $|y(\Upsilon)| < 2.4$, the $\Upsilon(nS)$ cross sections times dimuon branching fractions are found to be: $\sigma(pp \to \Upsilon(1S)X) \times B(\Upsilon(1S) \to \mu^+\mu^-) = (3.06 \pm 0.02^{+0.20}_{-0.18} \pm 0.12)$ nb, $\sigma(pp \to \Upsilon(2S)X) \times B(\Upsilon(1S) \to \mu^+\mu^-) = (0.910 \pm 0.011^{+0.055}_{-0.046} \pm 0.036)$ nb, and $\sigma(pp \to \Upsilon(3S)X) \times B(\Upsilon(3S) \to \mu^+\mu^-) = 0.490 \pm 0.010 \pm$

0.029 ± 0.020) nb. Here, the first uncertainty is statistical, the second is systematic and the third is associated with the integrated luminosity of the sample. Figure 2 shows that the cross sections are relatively flat as a function of rapidity until about 1.6 where they then fall quickly. The ratios of the differential cross sections for the $\Upsilon(nS)$ are also found to rise linearly as function of the transverse momentum of the Υ until about 20 GeV/c where they then become consistent with being constant. More information can be found in the reference [10].

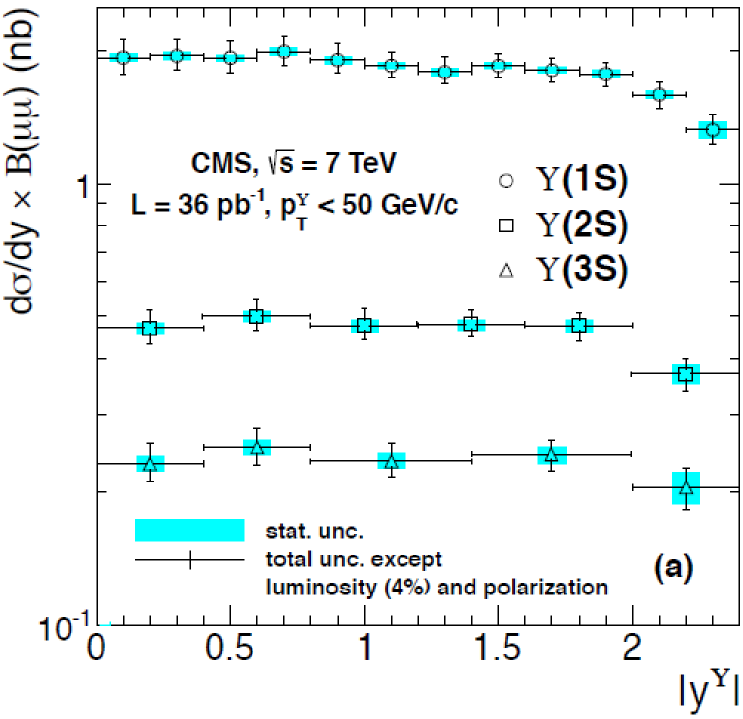

Figure 2: Acceptance-corrected differential production cross sections of the $\Upsilon(nS)$ as a function of rapidity. The bands represent the satistical uncertainty and the error bars represent the total uncertainty, except for those from the $\Upsilon(nS)$ polarization and integrated luminosity.

3 Search for a bottomonium state decaying to $\Upsilon(1S)\pi^+\pi^-$

An exotic charmonium state X(3872) has been observed by many including the CMS collaboration [11]. A theory for this state has not been established. Recently, the CMS collaboration has searched for the corresponding narrow bottomonium state (X_b) that would decay to $\Upsilon(1S)\pi^+\pi^-$ followed by $\Upsilon(1S) \to \mu^+\mu^-$ using a dataset of proton-proton collisions taken at a center of mass energy of 8 TeV that corresponds to an integrated luminosity of 20.65 fb^{-1}.

The reconstruction of the potential X_b meson and the normalization channel $\Upsilon(2S) \to \Upsilon(1S)\pi^+\pi^-$ starts with the reconstruction of the $\Upsilon(1S) \to \mu^+\mu^-$ and two oppositely charged pion candidates. Selection criteria are introduced that include the thresholds on transverse momenta, a mass window for the $\Upsilon(1S)$, quality requirements on kinematic fits, and requiring the minimum distance in the pseudorapidity and azimuthal angles to be small for the pions with respect to the $\Upsilon(1S)$ candidate momentum. The study was conducted in the kinematic region $p_T[\Upsilon(1S)\pi^+\pi^-] > 7.2$ GeV/c and $y[\Upsilon(1S)\pi^+\pi^-] < 2.0$. No significant signal is seen and an upper limit on the ratio of $\sigma[pp \to X_b \to \Upsilon(1S)\pi^+\pi^-]/\sigma[pp \times \Upsilon(2S) \to \Upsilon(1S)\pi^+\pi^-]$ is set in the range of 0.008-0.046 at the 95% confidence level [12].

4 Polarization studies for J/Ψ and Υ states

So far, the polarization of J/Ψ mesons is not satisfactorily described in the context of NRQCD. Here, the perturbative color-singlet production is complemented by possible nonperturbative transitions from colored quark pairs to the observable bound states. The high p_T quarkonia S-wave states directly produced are predicted to be transversely polarized with respect to the direction of their own momentum [13]. The CMS collaboration has studied the polarizations from prompt $\Upsilon(1S)$, $\Upsilon(2S)$, $\Upsilon(3S)$, J/Ψ, and $\Psi(2S)$ decays using a data sample collected at a center of mass energy of 7 TeV with integrated luminosity of 4.9 fb^{-1}.

The polarization of the $J^{PC} = 1^-$ states is measured through a study of the angular distribution from the decay to $\mu^+\mu^-$ using $W(\cos\theta, \phi|\overline{\lambda})\ \alpha\ \frac{1}{(3+\lambda_\theta)}(1+\lambda_\theta \cos^2\theta+\lambda_\phi \sin^2\theta \cos 2\phi+ \lambda_{\theta\phi} \sin 2\theta \cos\phi)$, where θ and ϕ are the polar and azimuthal angles, respectively, of the μ^+ with respect to the z axis of the chosen polarization frame. The three frame-dependent anisotropy parameters are extracted in three polarization frames and presented here for the center of helicity (HX) frame where the z axis coincides with the direction of the quarkonium momentum in the laboratory. Prompt decays are found by examining the proper time distribution. For the $\Upsilon(nS)$ states, Figure 3 shows for the rapidity range 0.0-0.6, one dimensional profiles of the polarization parameters as a function of the p_T of the Υ state and similar values are obtained for the 0.6-1.2 rapidity range [14]. Similarly, for the J/Ψ and $\Psi(2S)$ states, Figure 4 shows the distributions as a function of p_T for several $|y|$ bins [15]. All of the polarization parameters are compatible with zero or no transverse polarization. This is in disagreement with existing next-to-leading-order NRQCD theoretical expectations [16].

5 The Λ_b^0 lifetime

Using approximately 5 fb^{-1} of data collected in 2011, the Λ_b^0 lifetime was measured using the decay $\Lambda_b^0 \to J/\Psi\Lambda$ with $\Lambda \to p\pi^-$ and $J/\Psi \to \mu^+\mu^-$. Dimuon triggers optimised for selecting events with J/Ψ candidates were used. The four charged particles ($\mu^+\mu^-p\pi^-$) allow for a full reconstruction of the Λ_b^0 baryon. After particle quality cuts, kinematic vertex fits are used to find the Λ, the J/Ψ, and the proper decay time of the Λ_b^0 candidate. An unbinned extended maximum-likelihood fit is performed to determine the Λ_b^0 lifetime which uses the invariant mass of the Λ_b^0 candidate, the proper decay time and its uncertainty calculated per candidate. A projection of the invariant-mass and proper decay time distributions and the results of the fit is shown in Figure 5. Since the overall efficiency, determined through simulation, is consistent with being independent of the proper decay time, no efficiency correction is used. However, the largest systematic error is assigned to this source in addition to other systematic errors from alignment, event selection, and the fit model. The Λ_b^0 lifetime is found to be 1.503 ± 0.052 (stat.)± 0.031 (syst.) ps [17].

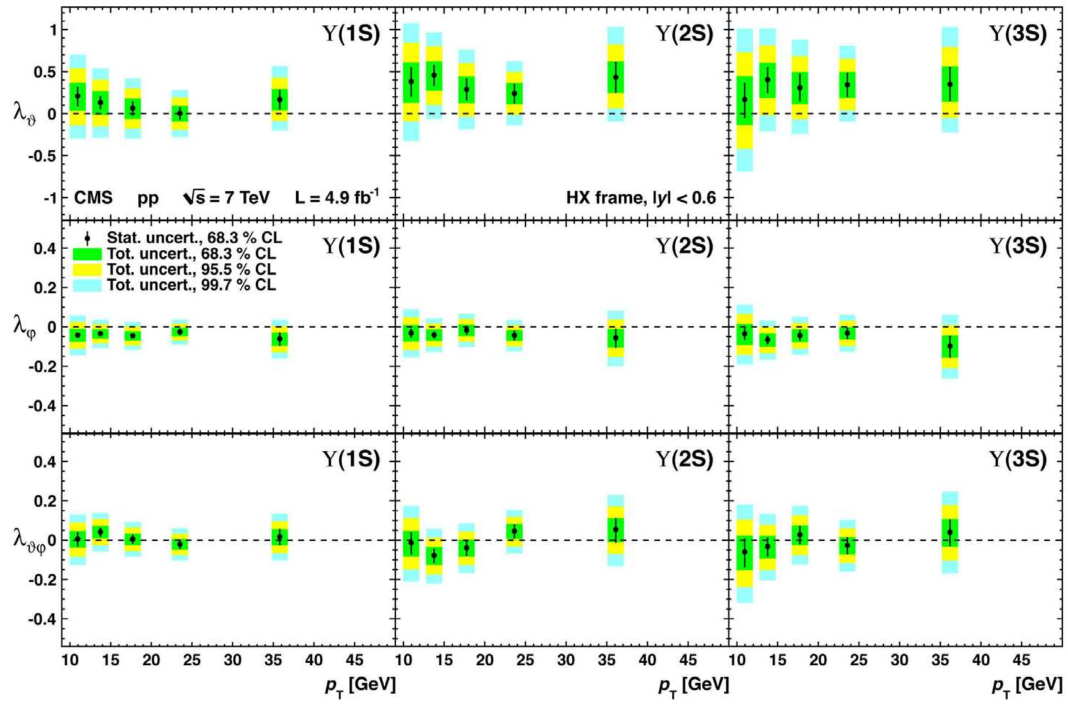

Figure 3: The λ_θ, λ_ϕ, and $\lambda_{\theta\phi}$ parameters (top to bottom) for the $\Upsilon(1S)$, $\Upsilon(2S)$, and $\Upsilon(3S)$ states (left to right), in the HX frame, for the rapidity $<$ 0.6 range. The bands represent 68.3, 95.5 and 99.7% C.L. intervals, while the error bars indicate the 68.3% C.L. interval when neglecting systematic uncertainties.

6 Observation of the decay $B_S \to \mu^+\mu^-$

A search for the rare decays $B_S^0 \to \mu^+\mu^-$ and $B^0 \to \mu^+\mu^-$ in pp collisions at center of mass energies of 7 and 8 TeV, with data samples corresponding to integrated luminosities of 5 and 20 fb^{-1}, respectively [19] is performed. At tree-level, flavor-changing neutral-current decays are forbidden in the standard model. However, these decays may proceed through higher-order loop diagrams so small branching fractions are predicted of $B(B_S^0 \to \mu^+\mu^-) = (3.57 \pm 0.30) \times 10^{-9}$ and $B(B^0 \to \mu^+\mu^-) = (1.07 \pm 0.10) \times 10^{-10}$ [18].

The search for the $B \to \mu\mu$ signal, where B denotes either B_S^0 or B^0, is performed in the dimuon invariant mass regions around the respective masses. The signal region was kept blind until all selection criteria were established. Selection variables included those which constrained isolated muons to a common vertex. The final selection is performed using boosted decision trees trained to distinguish between signal and background candidates. The combinatorial background is evaluated by extrapolating the data in nearby mass sidebands to the signal

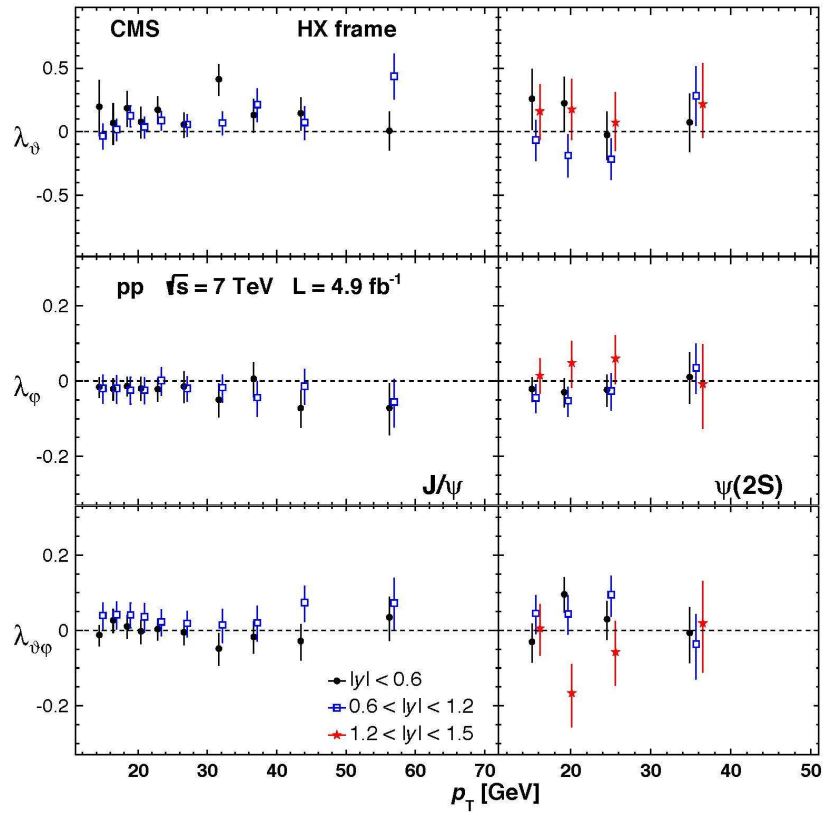

Figure 4: Measurements of the λ_θ, λ_ϕ, and $\lambda_{\theta\phi}$ parameters (top to bottom) for the J/Ψ (left) and $J/\Psi(2S)$ (right) in the HX frame, as a function of the $\Psi(nS)$ p_T for all rapidity ranges. The error bars represent the 68.3% C.L. total uncertainties.

region. Monte Carlo simulations are used to account for background from B and Λ_b decays. A normalization sample of $B^+ \to J/\Psi K^+ \to \mu^+\mu^- K^+$ decays is used. An unbinned maximum-likelihood fit to the dimuon invariant mass distribution gives a branching fraction $B(B_S^0 \to \mu^+\mu^-) = (3.0^{+1.0}_{-0.9}) \times 10^{-9}$, where the uncertainty includes both statistical and systematic contributions. An excess with respect to background of $B_S^0 \to \mu^+\mu^-$ is seen with a significance of 4.3 standard deviations. An upper limit at the 95% C.L. of $B(B^0 \to \mu^+\mu^-) < 1.1 \times 10^{-9}$ is determined. As can be seen from Figure 6, the results are in agreement with expectations from the standard model.

7 Acknowledgments

We congratulate our colleagues in the CERN accelerator departments for the excellent performance of the LHC and thank the technical and administrative staffs at CERN and at other CMS institutes for their contributions to the success of the CMS effort. In addition, we gratefully acknowledge the computing centres and personnel of the Worldwide LHC Computing Grid

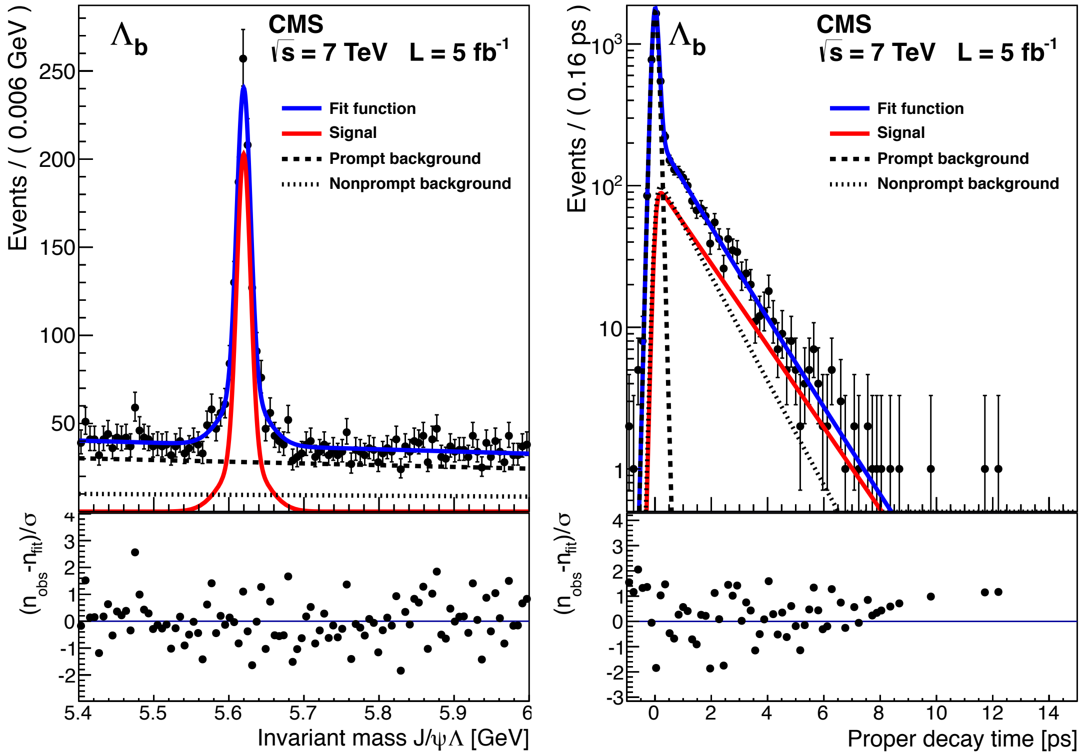

Figure 5: Projections of the invariant-mass and proper decay time distributions and the results of the fit are shown. The dark solid lines give the results of the overall fit to the data. The lighter solid lines are the signal contributions, and the dashed an dotted lines show the prompt and nonprompt background contributions, respectively.

for delivering so effectively the computing infrastructure essential to our analyses. Finally, we acknowledge the enduring support for the construction and operation of the LHC and the CMS detector provided by the following funding agencies: BMWF and FWF (Austria); FNRS and FWO (Belgium); CNPq, CAPES, FAPERJ, and FAPESP (Brazil); MES (Bulgaria); CERN; CAS, MoST, and NSFC (China); COLCIENCIAS (Colombia); MSES (Croatia); RPF (Cyprus); MoER, SF0690030s09 and ERDF (Estonia); Academy of Finland, MEC, and HIP (Finland); CEA and CNRS/IN2P3 (France); BMBF, DFG, and HGF (Germany); GSRT (Greece); OTKA and NKTH (Hungary); DAE and DST (India); IPM (Iran); SFI (Ireland); INFN (Italy); NRF and WCU (Republic of Korea); LAS (Lithuania); CINVESTAV, CONACYT, SEP, and UASLP-FAI (Mexico); MBIE (New Zealand); PAEC (Pakistan); MSHE and NSC (Poland); FCT (Portugal); JINR (Dubna); MON, RosAtom, RAS and RFBR (Russia); MESTD (Serbia); SEIDI and CPAN (Spain); Swiss Funding Agencies (Switzerland); NSC (Taipei); ThEPCenter, IPST, STAR and NSTDA (Thailand); TUBITAK and TAEK (Turkey); NASU (Ukraine); STFC (United Kingdom); DOE and NSF (USA). In particular, this work was supported by the PIRE

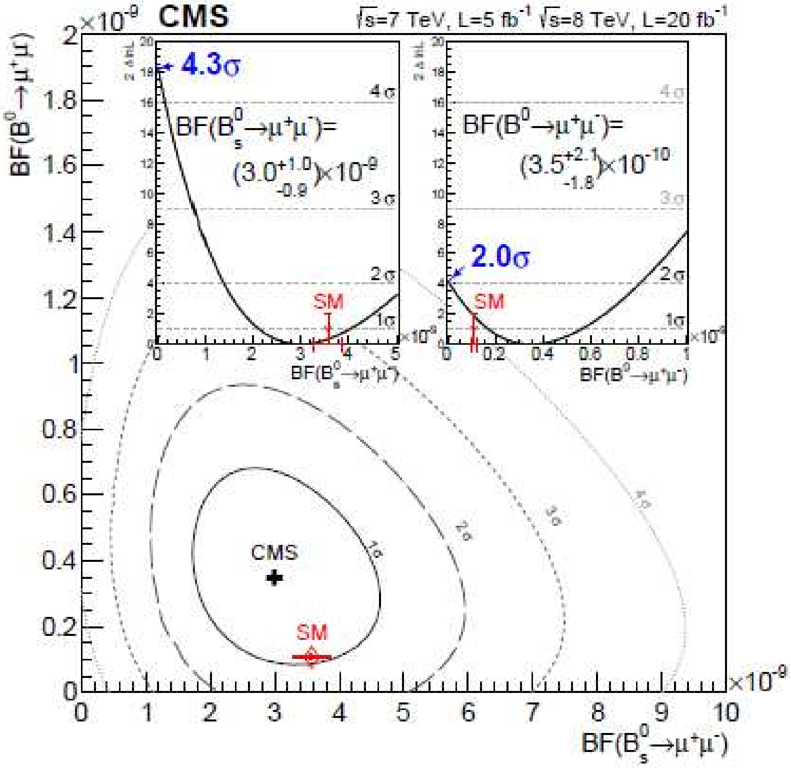

Figure 6: Categorized boosted decision tree scan of the ratio of the joint likelihood $B(B_S^0 \to \mu^+\mu^-)$ and $B(B^0 \to \mu^+\mu^-)$. The insets show the likelihood ratio scan for each of the branching fractions when the other is profiled together with other nuisance parameters. The significance at which the background-only hypothesis is rejected is also shown.

Grant OISE-0730173 of the US-NSF.

References

[1] P. Nason, S. Dawson, and R.K. Ellis, Nucl. Phys. **B303** 607 (1988); M. Cacciari, M. Greco, and P. Nason, JEHP **05** 007 (1998); B.A. Kriehl, G. Kramer, I Schienbein *el al.*, Phys. Rev. **D77** 014011 (2008).

[2] CMS Collaboration, Phys. Lett. **B714** 136 (2011).

[3] CMS Collaboration, Phys. Rev. Lett. **106** 112001 (2011).

[4] CMS Collaboration, Phys. Rev. Lett. **106** 252001 (2011).

[5] CMS Collaboration, Phys. Rev. D **84** 052008 (2011).

[6] M Cacciari and M. Greco, Nucl. Phys. **B421** 530 (1994); M. Cacciari, M. Greco, and P. Nason, JHEP **05** 007 (1998); S. Alioli *et al.*, JHEP **06** 043 (2010); S. Frixione, P. Nason, and G. Ridolfi, JHEP **09** 126 (2007).

[7] G.T. Bodwin, E. Braaten, and G.P. Lepage, Phys. Rev. **D51** 1125 (1995).

[8] S. Chatrchyan *et al.* (CMS Collaboration), JINST **3** S08004 (2008).

[9] N. Brambilla *et al.*, Phys. J. **C71** 1534 (2011);

[10] CMS Colaboration, arXiv:1303.5900 (2013), to be published in Phys. Lett. B.

[11] CMS Collaboration, JHEP **04** 154 (2013).

[12] CMS Collaboration, arXiv:1309.0250 (2013), submitted to Phys. Lett. B.

[13] J.-P. Lansberg, Eur. Phys. J. **C61** 693 (2009); M. Beneke and M. Kramer, Phys. Rev. **D55** 5269 (1997); A.K. Leibovich, Phys. Rev. **D56** 4412 (1997); E. Braaten, B.A. Kniehl, and J. Lee, Phys. Rev. **D62** 094005 (2000).

[14] CMS Collaboration, Phys. Rev. Lett. **110** 0818022 (2013).

[15] CMS Collaboration, arXiv:1307.6070 (2013), to be published in Phys. Lett. B.

[16] B. Gong, J.-X. Wang, and H.-F. Zhang, Phys. Rev. **D83** 114021 (2011); P. Artoisenet, J. Campbell, J.P. Lansbert, F. Maltoni, and F. Tramontano, Phys. Rev. Lett **101** 152001 (2008); M. Butenschoen and B.A. Kniehl, Phys. Rev. Lett. **108** 172002 (2012); B. Gong, L.-P. Wan, and H.-F. Zhang, Phys. Rev. Lett. **110** 042002 (2013).

[17] CMS Collaboration, JHEP **07** (2013);

[18] A.J. Buras, J. Girrbach, D. Guadagnoli, and G. Isidori, Eur. Phys. J. **72** (2012); K. De-Bruyn *et al.*, Phys. Rev. Lett. **109** 041801 (2012).

[19] CMS Collaboration, Phys. Rev. Lett. **111** 101804 (2013).